Modeling turbulent impurity transport in the SOL of DIII-D with a reduced model

S. Zamperini[a*], J.H. Nichols[b], T. Odstrcil[c], T. Abrams[a], J.A. Boedo[d], J.D. Elder[e], D.L. Rudakov[d], D.C. Donovan[f], J.D. Duran[b], A. Huang[g]

[a]*General Atomics, San Diego, CA,* [b]*Oak Ridge National Laboratory, Oak Ridge, TN,*
[c]*Massachusetts Institute of Technology, Cambridge, MA,*
[d]*University of California, San Diego, CA,* [e]*University of Toronto, Toronto, Canada,*
[f]*University of Tennessee, Knoxville, TN,* [g]*University of California, Santa Barbara, Santa Barbara, CA*

[*]Corresponding author: zamperinis@fusion.gat.com

Abstract

A novel impurity transport model that approximates SOL turbulence as a fluctuating poloidal electric field is shown to be an acceptable replacement for the traditional approach of assigning an arbitrary radial diffusion coefficient to the impurity ions. The model is implemented in the DIVIMP impurity transport code and applied to an L-Mode tungsten divertor experiment on DIII-D. The poloidal electric field is represented as fluctuating between ±1,000 V/m based on previous measurements. The resulting intermittent $v_r = E_\theta \times B_T$ transport causes ions to transport both into the core as well as into the far-SOL. Simultaneous agreement with estimates of the W density just inside the separatrix as well as in the far-SOL is obtained ($n_W \sim 10^{14}$ m^{-3} and $n_W \sim 10^{12}$ m^{-3}, respectively). Prompt re-deposition of the W ions was necessary to obtain agreement ($f_{redep} \sim 99\%$). We conclude that simulating impurity transport using a physics-based approximation for turbulence in the SOL, versus arbitrarily assigning diffusion coefficients, may enable better reactor scale predictions of core impurity contamination.

I. Introduction

If the core of future tokamak-based fusion reactors contains too many impurities, then it may be unable to reach Q=1 and may even result in a damaging disruption. Impurities are sourced from the intense plasma-material interactions at the vessel walls and reach the core by transporting through the scrape off layer (SOL) as ions. SOL impurity transport is typically divided into parallel-to-B transport and radial transport. Parallel transport explains how impurities escape the divertor region and transport around the SOL. Parallel transport is on relatively firm theoretical footing and is readily understood in terms of the 1D parallel fluid equations (Ch. 6 of [1]), but ultimately it is the radial transport of impurities that moves them into the core. Unfortunately, radial impurity transport lacks a firm theoretical underpinning and is often treated as diffusive with transport coefficients on the order of $D_\perp \sim 0.01\text{-}10$ m^2/s. To date, there is no theory that explains the use of such "anomalous" diffusion coefficients. Classical and neoclassical diffusion predicts diffusion coefficients that are around 3-5 orders of magnitude too small, and it is not clear if neoclassical effects are valid in the SOL. Bohm diffusion ($D_\perp = 0.06T_e/B$ [1]) calculates values of the correct order of magnitude in the near-SOL, but it is derived for the main ions (deuterium) in

non-toroidal plasmas; there is little/no evidence that it is appropriate to use in tokamaks [1][2]. Furthermore, the direct relationship with T_e is in stark disagreement with experimental measurements since it is well-established that $D_\perp$, when extracted from measured radial profiles of n_e, increases in the colder far-SOL [3]. Therefore, unless a theory for such large diffusion coefficients in the SOL emerges, the current estimates of $D_\perp$ in 2D fluid models, while convenient for interpreting experimental measurements, cannot be considered physics-based.

Current reactor designs often assume a user-prescribed $D_\perp$ for the SOL (e.g., linearly increasing towards the wall in SPARC [4] or 1 m^2/s for Be transport in ITER [5]) despite little reason to believe the values that reproduce measurements in today's machines, which already vary over three orders of magnitude, will hold for reactor-scale conditions. This means reactor scale predictions of core impurity contamination are dubious, and brings into question the successful operation of the reactor.

It is widely accepted that radial plasma transport of the main ions as well as the impurities is likely due to turbulence. Turbulence is a broadly used term that includes microscopic (~um's) and macroscopic (~cm's) fluctuations in plasma parameters such as the plasma density, temperature or the electric field. Despite the extremely encouraging results from recently developed Braginskii-fluid [6] and gyrokinetic SOL codes [7], modeling turbulent phenomena remains notoriously difficult and computationally expensive due to the wide range in the spatial and time scales. Reduced models can fill in the knowledge gap between the prevalent, yet arbitrary, prescription of radial diffusion and full-scale turbulence modeling of impurities.

Consequently, in this paper we ask if a reduced radial impurity transport model based on fluctuating plasma quantities can be developed that reproduces experimental measurements of impurities within the SOL of DIII-D. Specifically, we consider a model based on previous measurements of fluctuations in the poloidal electric field, E_θ, in the SOL and the resulting radial drift ($v_r = E_\theta \times B_T$) on the impurity ions. We implement the model in the 2D Monte Carlo impurity transport code DIVIMP and test it on tungsten transport experiments carried out during the 2016 DIII-D Metal Rings Campaign [8]. The results are benchmarked against experimentally constrained measurements of W density within the core by TGYRO [9] and in the far-SOL by 3DLIM [10]. We find that a radial transport model based on fluctuations in E_θ can reproduce the expected radial profile of W density at the outboard midplane of DIII-D.

II. Materials and Methods

a. Simple L-mode Discharge during the DIII-D Metal Rings Campaign

The Metal Rings Campaign (MRC) was carried out on DIII-D in the summer of 2016. We focus on DIII-D discharge #167196 in this publication because it was a highly diagnosed "simple as possible" [11] MRC discharge and has already been analyzed and modeled extensively in previous publications [10][12][13][14]. This is a stationary L-mode discharge with 3.2 MW of injected power and a line-averaged density of 3.2×10^{19} m^{-3}. A schematic of the experimental layout relevant to this publication is shown in Figure 1a). Two toroidally symmetric W rings were installed in the lower, open divertor as shown in cyan. The strike point was stationed on the upper ring located on the lower divertor shelf. Langmuir probes measured the plasma density (n_e) and temperature (T_e)

at the outer target. Thomson scattering measured n_e and T_e upstream of the target along the indicated chord. A fast-plunging reciprocating Langmuir probe (RCP) [15] measured n_e, T_e and the parallel-to-B plasma Mach number near the midplane. Figure 1b) shows the tungsten erosion from the upper ring. It was measured via a filtered photomultiplier filterscope and a filtered camera both monitoring the W-I 400.9 nm line [16]. W-I emission intensities were converted to gross erosion fluxes using the ionizations/photon (S/XB) method [17].

The different regions in Figure 1 are color-coded according to where each code, to be introduced in this section, is applicable: TGYRO in the core (red), DIVIMP and OSM-EIRENE in most of the SOL (pink) and 3DLIM in the very far-SOL (green). We maintain these color conventions within the plots in this paper.

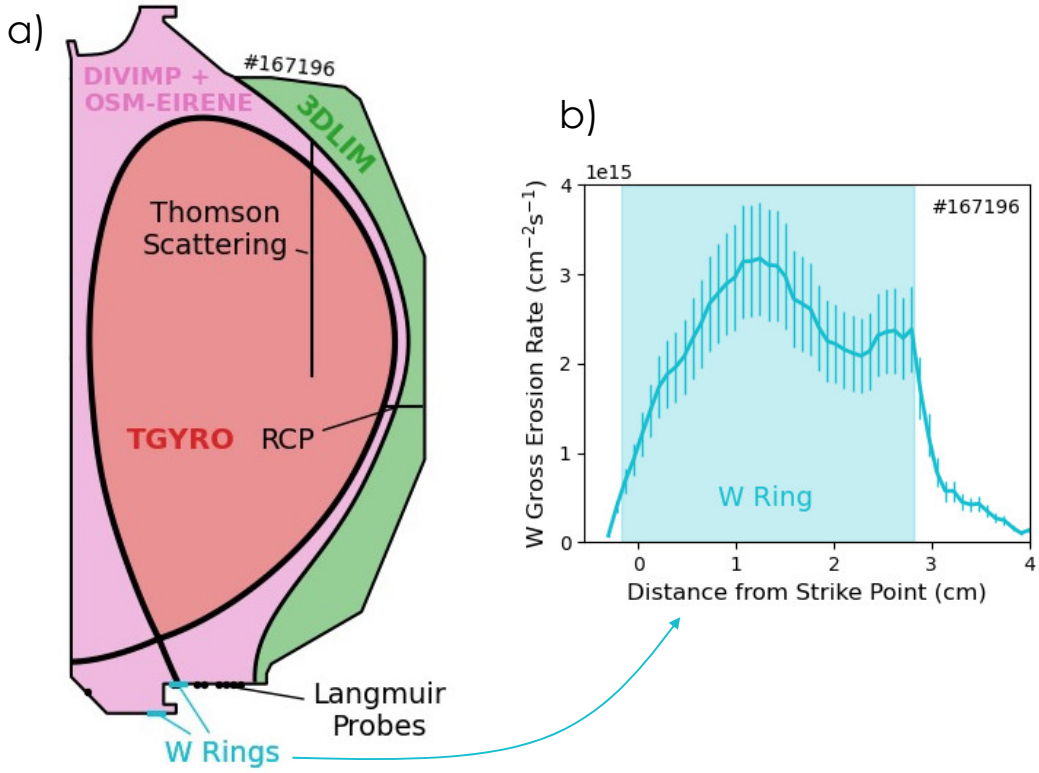

Figure 1. a) Cross section of DIII-D discharge #167196. Regions are color-coded according to where each code referenced in this study is applicable. The location of the Thomson scattering and RCP measurements are indicated. The W rings are located at the lower divertor. b) The measured erosion profile of the upper ring is indicated (reproduced from [13]).

b. TGYRO

Core impurity transport was modeled by the TGYRO solver [9]. TGYRO combines TGLF-SAT0 [18] and NEO [19] code to predict heat and particle fluxes and integrates steady-state transport equations to calculate temperature and density profiles matching these fluxes. *The tungsten transport was modeled by adding two trace species. Because the turbulent transport is weakly dependent on impurity charge, all W ions were represented by a single species with charge Z = 40 and mass 183 amu. Z = 40 was chosen since it is equal to the average W charge in the plasma core. One trace species has a zero-density gradient. The other has a nonzero gradient and 0.1%*

higher Z, to avoid numerical issues in TGLF. Since the gradient-flux relation for trace species is linear, the difference in the fluxes of these traces allows us to determine the zero-flux gradient of total tungsten density and integrate the steady-state profile. The absolute scale of the tungsten density profile is the integration constant and needs to be determined experimentally from the measured tungsten density. The scale is estimated from measured SXR emission after subtraction of bremsstrahlung from low-Z ions. The remaining part of SXR emission is proportional to tungsten density, electron density, and tungsten SXR cooling coefficients, describing how much W radiates at a given electron temperature.

c. OSM-EIRENE

OSM-EIRENE solves the 1D plasma fluid equations in the SOL as defined in Ch. 9-11 of [1] and iterates the solution with the kinetic Monte Carlo neutral transport code EIRENE to account for neutral ionization and recombination sources ([20], but see [14] for a modern example). As an interpretive code, it reconstructs the deuterium plasma background using experimental data as input, in this case n_e and T_e at the targets, and uses experimental data from elsewhere in the SOL to constrain the solution. In this study, Langmuir probe n_e and T_e data at the target is input to OSM-EIRENE, and the resulting plasma reconstruction is compared against the Thomson scattering n_e and T_e data as well as the RCP n_e, T_e and Mach number measurements. To obtain sufficient agreement with experiment, user-defined functions of experimentally unknown momentum sources from neutrals and impurities near the target are prescribed. The code assumes toroidal symmetry, and thus the result is a 2D radial-poloidal reconstruction of the discharge.

DIII-D is a graphite-walled device that routinely operates with carbon concentrations on the order of 2%. OSM-EIRENE does not explicitly include the impact of carbon on the plasma reconstruction, though by virtue of user-modifications to the momentum and radiation sources to obtain agreement with experimental data, the effects are implicitly included. Such a process is common in interpretive code workflows.

d. DIVIMP

DIVIMP is a 2D Monte Carlo impurity transport code used to track the transport and calculate the density of impurity ions in the SOL [20]. It operates under the "trace impurity approximation," which states that the impurity concentration is sufficiently low enough that it has a negligible effect on the background plasma. TGYRO simulations carried out on #167196 indicate a core W concentration of $c_W \sim 10^{-4}$ near the separatrix, which we take as a reasonable indication that the trace impurity approximation applies. DIVIMP tracks impurities in a steady-state plasma background, which, in this study, is provided by OSM-EIRENE. DIVIMP accepts the experimentally inferred W erosion as input. The W neutral and ion ionization/recombination rates are calculated using the ADAS database [21]. The plasma background is used to calculate the parallel forces on the impurity ions (Ch. 6 of [1]). Radial transport is historically treated as diffusive, though in this section we propose an alternative to the diffusive treatment. The net transport of each ion is calculated at a user-specified timestep, $\Delta t = 10^{-7}$ s in this study. Impurity ions are tracked until they leave the simulation grid or are deposited on a vessel surface. After tracking many ions (~10,000-100,000) DIVIMP uses standard Monte Carlo techniques to calculate the steady-state impurity density throughout the simulation grid.

For this study DIVIMP was upgraded to include a novel fluctuation based radial transport model and an ERO code-based scaling of W prompt redeposition during MRC to better describe W transport and sourcing in the SOL. We describe each of these upgrades below.

i. Fluctuation Model

To implement SOL impurity transport in a more physically justifiable way, a reduced model of intermittent radial impurity transport based on fluctuations in E_θ ($v_r = E_\theta \times B_T$) was implemented in DIVIMP. The user manually inputs a table of values where each row consists of the normalized poloidal flux value of the flux tube, Ψ_N, the magnitude of the fluctuating E_θ and the probability that the fluctuation is a positive value, p^+. A "correlation time," τ_{corr}, is also specified. The implementation occurs during every timestep as follows:

1. A value of E_θ is chosen from the table based on the ion's Ψ_N value. If there is no matching Ψ_N value, then E_θ is linearly interpolated between the two bounding Ψ_N values.
2. The sign of E_θ is randomly chosen using the corresponding value of p^+. This value is also linearly interpolated if necessary.
3. The ion travels in the radial direction at a velocity $v_r = E_\theta \times B_T$ for τ_{corr} seconds before another E_θ is sampled.

In the counter-clockwise toroidal field magnetic configuration of #167196, positive values of E_θ result in radially outward transport. In theory, the statistics of E_θ fluctuations from the RCP can be analyzed and used as direct input to the model. In this study we take a simpler approach and enter a single table entry for Ψ_N, E_θ and p^+. Since there is only one entry, the values for E_θ and p^+ are interpreted as SOL-wide averages in order to demonstrate a proof-of-concept of the model. Data on E_θ in the SOL is scarce, though visual inspection of the RCP E_θ signal for the DIII-D L-Mode discharge in Fig. 3 of [23] indicates values in the range of ±1,000 V/m are reasonable. It is not clear if the fluctuations tend toward positive or negative. Therefore, the fluctuation magnitude and probability of a positive fluctuation value are E_θ = 1,000 V/m and $p^+ = 0.5$. The correlation time was $\tau_{corr} = 3$ μs. τ_{corr} can be interpreted as an approximation as the duration of a plasma fluctuation from the frame of the impurity ion. This could include the effect of a passing "blob" (see section IV).

ii. Prompt re-deposition

Prompt redeposition of sputtered W atoms in DIVIMP is necessary when considering absolute magnitudes of W density within the SOL. The probability of a W ion *not* promptly re-depositing is described by the ERO scaling in [24] and experimental validation in [25]:

$$p = 1 - f_{redep} = e^{-\alpha x^\beta}$$

α and β are free parameters. x is defined as $x = \lambda_{iz}/\lambda_{sheath}$, where λ_{iz} is the characteristic ionization length for a neutral W atom, and λ_{sheath} is the thickness of the magnetic presheath. A fit to ERO simulations determined α=1.485 and β=-0.56. For typical attached DIII-D divertor conditions, this

results in around ~99% of the eroded W atoms promptly redepositing. As discussed below, significant W prompt re-deposition greatly improves the agreement between DIVIMP, TGYRO, and 3DLIM calculations of W density at the border between each code's respective region of validity.

e. 3DLIM

3DLIM is a Monte Carlo SOL impurity transport code similar to DIVIMP, except it is a full 3D code and is only suited for far-SOL studies due to its more simplistic plasma solver. As a 3D code it is better equipped to handle the 3D geometry of the DIII-D wall compared to OSM-EIRENE/DIVIMP, which previous studies have shown can have first order effects on impurity transport near the wall [10]. In [10] 3DLIM was successfully used to reproduce collector probe deposition patterns for probes inserted in the same discharge as the one we consider here. By reproducing W deposition patterns on the collector probes, the transport properties of the W ions in the far-SOL were inferred. The study found that W ions in the far-SOL were not compatible with radial diffusive transport model and likely traveled convectively in the radial direction at about v_r = 500 m/s. A similar conclusion was found much earlier on Alcator C-Mod during He-3 experiments [22]. The results of both these studies partially motivate the current study finding alternatives to diffusive radial transport in impurity SOL codes. Here we adapt the already constrained 3DLIM simulations from [10] by removing the collector probe from the simulations to infer the unperturbed W density in the far-SOL region (green region in Figure 1).

III. Results

a. OSM-EIRENE Plasma Reconstruction

The OSM-EIRENE plasma reconstruction is sufficiently constrained by the Thomson scattering and RCP data, Figure 2. Due to uncertainties in the separatrix location and mapping to the plasma coordinates, the Thomson data was shifted radially outwards by $\psi_n = 0.03$ and the RCP data shifted inwards by 1.5 cm so that agreement between the two diagnostics could be obtained (not shown). OSM-EIRENE is in reasonable agreement with the Thomson scattering T_e and n_e data, as shown in Figure 2a) and 2b), respectively. The agreement with the RCP T_e, n_e and Mach number data is also reasonable, Figures 2d)-f). It must be noted that in OSM-EIRENE the Mach probe data is input directly to OSM-EIRENE; that is, the correct flow pattern at the midplane is imposed ad-hoc and is not self-consistently solved from the 1D fluid equations (as has been done previously [26][27]). At the time of this experiment the LLAMA diagnostic [28], which infers neutral density via Lyman-alpha emission, had not yet been installed. Nonetheless, the simulated neutral density at the location of LLAMA is included Figure 2c) to demonstrate it as an important part of the constraining process. This plasma reconstruction is passed into DIVIMP to obtain the impurity density results in the following section.

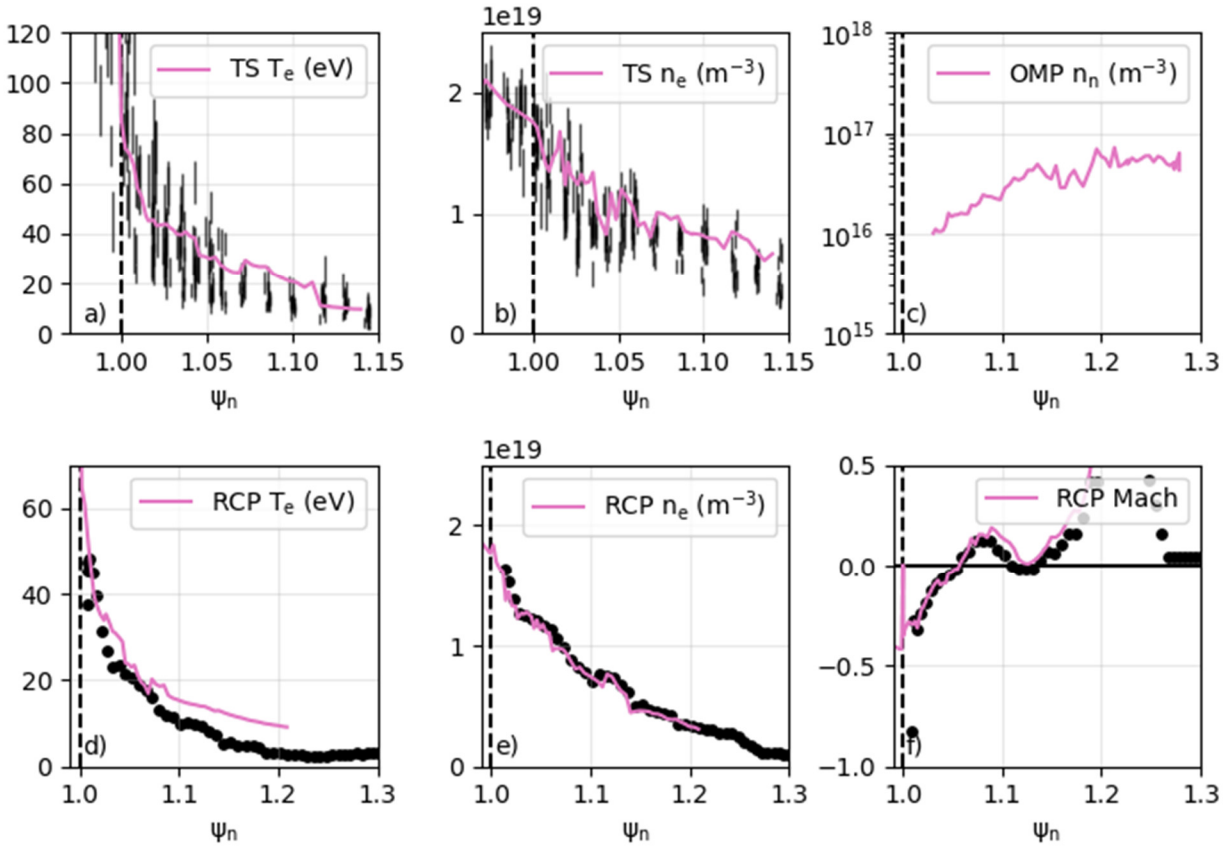

Figure 2. OSM-EIRENE (pink) compared against experimental data (black). Thomson scattering T_e (a) and n_e (b). Neutral density at the location of LLAMA, but LLAMA was not installed yet (c). RCP T_e (d), n_e (e) and Mach number (f).

b. TGYRO/DIVIMP/3DLIM Calculations of Tungsten Density

The 2D cross section of the W density calculated with DIVIMP is shown in Figure 3. Compared to the far-SOL, Figure 3 unsurprisingly shows larger amounts of W in the near-SOL since that is

where the W ring is, but in order to make a more quantitative assessment of the W transport results we narrow our focus to the density at the outboard midplane.

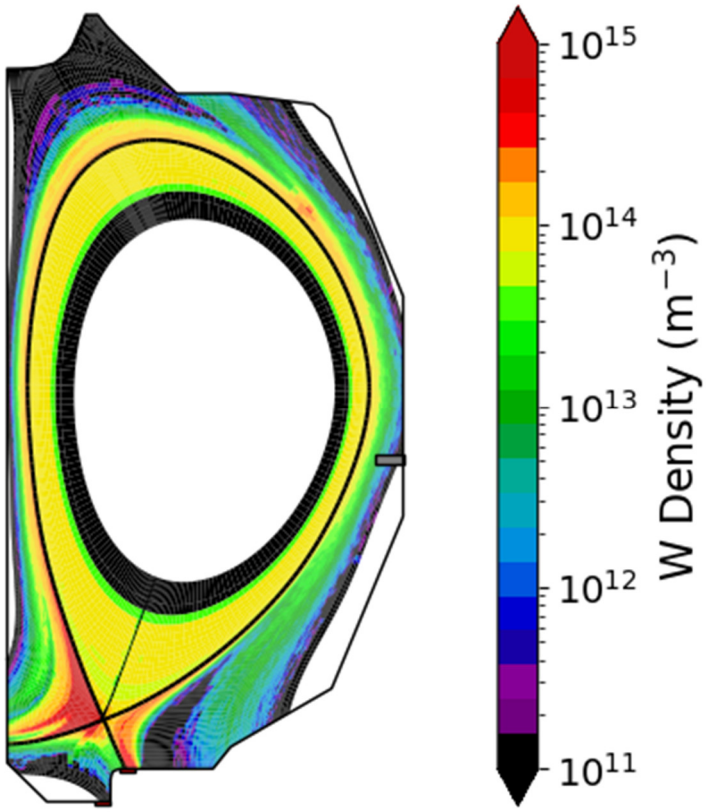

Figure 3. 2D cross section of a DIVIMP simulation of W density in DIII-D discharge #167196 using the fluctuation-based radial transport model.

Acceptable agreement in the W densities simulated by each code at the outboard midplane is found, Figure 4. In the core region (red) the TGYRO results, which are constrained by SXR data, show a relatively flat W density profile. Results from two different DIVIMP simulations are shown. The fluctuation-based model is plotted as the solid pink line, and a repeat simulation where the radial impurity transport is treated as diffusive with $D_\perp = 0.3$ m^2/s is plotted as the black/pink dashed line. Both simulations are within a factor of 2× with the TYGRO data in the core. The diffusive simulation has better agreement with the 3DLIM results (green) in the far-SOL, though the fluctuation-based results are still within a factor of ~4× agreement. This is likely due to using a SOL-wide average for the fluctuating E_θ. Experimentally, E_θ is smallest in the far-SOL therefore a more rigorous treatment would use values smaller than 1,000 V/m in the far-SOL. Smaller values would decrease the net radial transport and thus the density in the far-SOL (see the E_θ scan results in Figure 5b)).

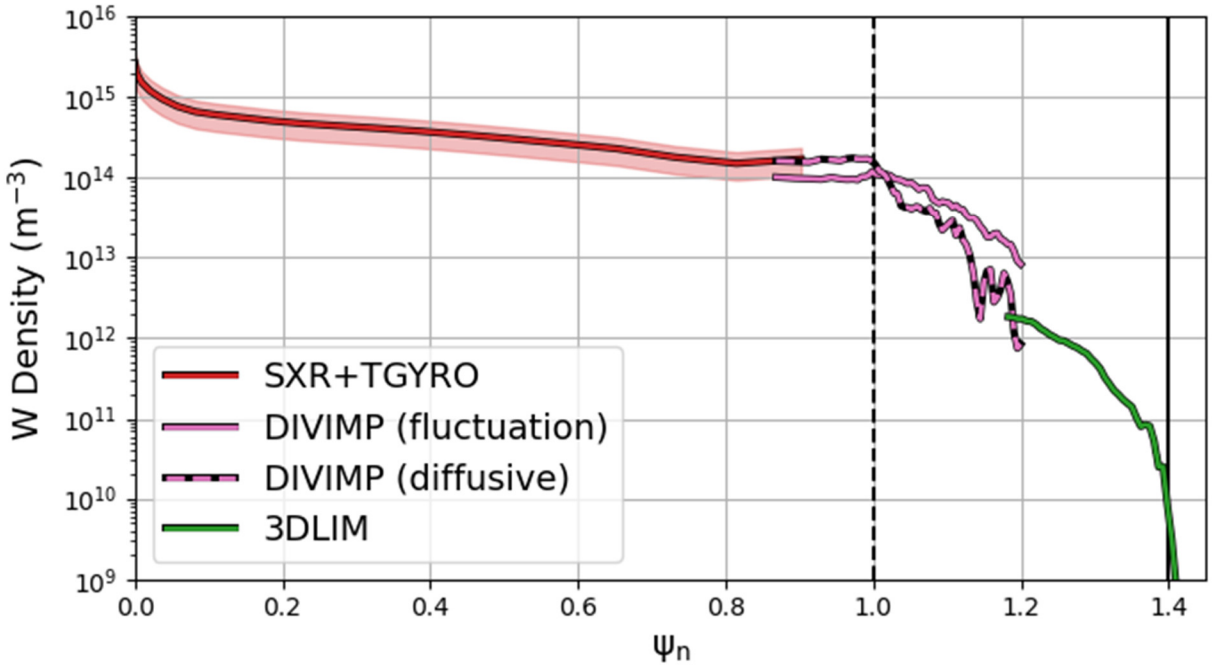

Figure 4. Core-to-wall modeling results of W density at the outboard midplane of #167196. TGYRO simulates W density in the core (red, with light red error band), DIVIMP in most of the SOL (pink) and 3DLIM in the very far-SOL (green).

c. Parameter Scans in Fluctuation Model Inputs

Parameters scans in E_θ, p^+ and τ_{corr} were performed to assess the sensitivity of the results to each parameter: E_θ was varied from 100 – 2,000 V/m with $p^+ = 0.5$ and $\tau_{corr} = 3$ μs, p^+ was varied from 0.4 – 0.6 with E_θ = 1,000 V/m and $\tau_{corr} = 3$ μs, and τ_{corr} was varied from 0.1 – 10 μs with E_θ = 1,000 V/m and $p^+ = 0.5$. The E_θ scan is shown in Figure 5a), the p^+ scan in Figure 5b) and the τ_{corr} scan in Figure 5c). Increasing E_θ above 1,000 V/m had a negligible impact on the results, though below 1,000 V/m the results proved to be particularly sensitive. In particular, values below 1,000 V/m led to disproportionately large decreases in the W density within the core. p^+ is shown to be a particularly sensitive parameter as well. For values $p^+ < 0.5$, i.e., when the probability of inward transport is larger than outward transport, the core W density increased by well over an order of magnitude relative to $p^+ = 0.5$. Conversely, for values above $p^+ = 0.5$, the core W density decreases by about 1 or 2 orders of magnitude due to increased likelihood of transport in the SOL being away from the core. If p^+ is increased above ~0.6 or below ~0.4, a negligible amount of W escapes from the divertor region and very little reaches the core (not shown). The τ_{corr} scan showed little variation when τ_{corr} was increased above 3 μs, but decreasing below 3 μs eventually led to a steep drop off in the far-SOL W density.

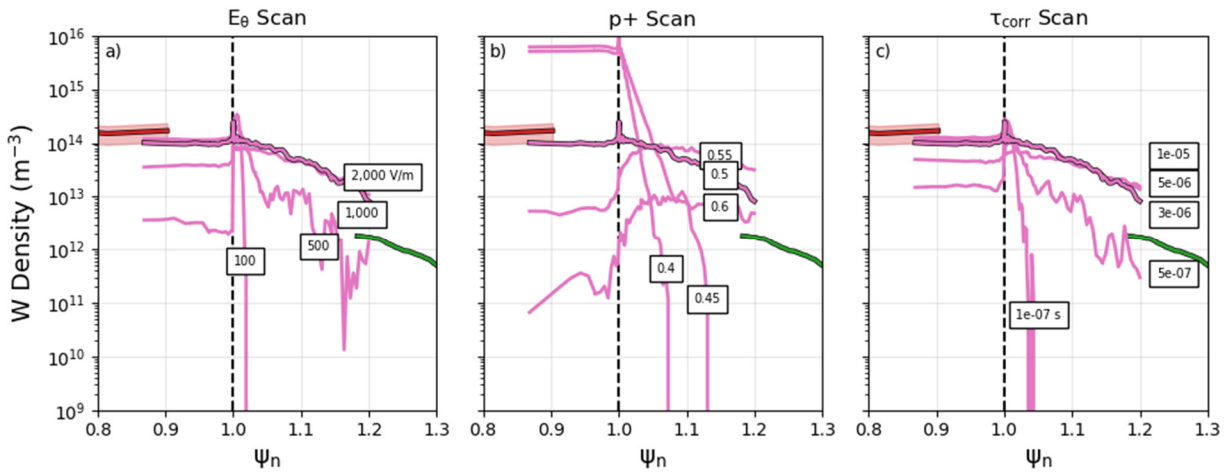

Figure 5. a) W density calculations from DIVIMP during a scan in E_θ from 100 – 2,000 V/m. b) Scan in p^+ from 0.4-0.6. c) Scan in τ_{corr} from 0.1 to 10 μs.

IV. Discussion

a. Fluctuations in E_θ as an Explanation for Radial SOL Impurity Transport

A reduced model for the fluctuating poloidal electric field is a physically justifiable replacement for diffusive impurity transport within DIVIMP. It simultaneously obtains agreement with experimentally constrained TYGRO and 3DLIM W density calculations at the outboard midplane to within a factor of 2-4×. The results are very similar to a diffusive transport prescription, but we remind the reader that there is no physical theory that explains diffusion coefficients as large as $D_\perp = 0.3$ m^2/s in the SOL. Considering the fluctuation-based model is meant to act as a reduced model for SOL turbulence, it may be hypothesized that diffusive models are simply approximating the net result of intermittent bi-directional transport from fluctuations in E_θ.

The scan in E_θ demonstrates that the magnitude of E_θ can have a significant impact on the core W density. As E_θ increases the impurity density profile in the SOL flattens due to increased radial transport velocities. This is accompanied by an increase in the core W density, at least up until around 1,000 V/m. It is not immediately clear why the curves for 1,000 and 2,000 V/m in Figure 5a) are essentially identical. This seems to point towards a "saturation" type effect in this parameter, though further inspection is needed. Regardless, from a core-edge integration perspective it may be desirable to consider scenarios in which E_θ fluctuations near the separatrix are kept to a minimum to prevent the associated inward transport of impurities into the core.

The p^+ scan demonstrates that W density within the core is likewise very sensitive to p^+. At values of $p^+ < 0.5$, i.e., a bias towards negative E_θ values and the associated inward transport that it causes, the core W density unsurprisingly increases. The opposite is observed for $p^+ > 0.5$. This suggests that for core-edge integration, it is desirable that the fluctuations in E_θ tend to be more positive than negative. This is the same as requiring positive skewness of the probability distribution function of E_θ fluctuations, as measured by an RCP or even beam emission spectroscopy (BES)

[29]. This results in the desirable scenario in which impurities are preferentially sent towards the vessel wall instead of the core where they can harm performance.

It may be observed that while $E_\theta \times B_T$ impurity transport towards larger R should decrease core contamination at the outboard midplane, this same transport at the inboard midplane would move impurities into the core. Qualitatively speaking, the unfavorable curvature at the outboard midplane would result in more turbulent MHD activity, which may translate to larger fluctuations in E_θ. This is compounded by the observation that impurities may accumulate near the outboard midplane in certain magnetic configurations, providing a localized source of impurities into the core [14][27]. Therefore, while core contamination from the inboard side is fully deserving of dedicated research, it is reasonable to focus on transport at the outboard midplane as it is likely where the largest number of impurities cross the separatrix.

The correlation time in these simulations $\tau_{corr} = 3$ μs is on the order of what it is expected if we consider the typical size and speed of turbulent density "blobs" in the SOL. Blobs are intermittent turbulent structures born from the interchange instability near the separatrix and are the largest regularly observed turbulent structure in the SOL [30]. They can be considered as a traveling coherent E_θ perturbation with values in DIII-D on the order of very roughly ~1,000 V/m. They are typically around 1 cm wide in the radial direction and travel at their drift velocity $v_r = E_\theta \times B_T$ [23], i.e., around 1,000 m/s radially outwards. The transit time to pass a given point in space is thus very roughly approximated as 0.01/1000 = 10 μs. Assuming similar transit velocities for the smaller plasma fluctuations, τ_{corr} should decrease due to the smaller sizes. Therefore, since the reduced model in DIVIMP condenses all the physics of turbulent E_θ fluctuations into an average value, $\tau_{corr} = 10$ μs should be considered an upper limit. Trial and error lead to $\tau_{corr} = 3$ μs as the best match to the boundary conditions imposed by TGRYO and 3DLIM. This value is close to, but less than, the upper limit approximated by blobby transport.

Because a single value for E_θ, p^+ and τ_{corr} are used for the entire SOL in the best-match DIVIMP simulation in Figure 4, they are appropriately interpreted as a SOL-wide set of average values that reproduce experimentally constrained data from TGYRO and 3DLIM. In the actual experiment the magnitude of the fluctuations and ratio of positive/negative fluctuations certainly varies throughout the SOL. As discussed above, a more sophisticated approach would involve radially varying profiles of E_θ and p^+, such as larger values for E_θ near the separatrix and smaller values in the far-SOL. This seemingly introduces a paradox: experimentally it has long been observed that anomalous diffusion coefficients increase in the far-SOL, which one would intuitively think would require larger values of E_θ in the far-SOL, not smaller. The disparity is likely due to the approximations in the model, as it only considers an approximation to the turbulent-like $E_\theta \times B_T$ drift. Other drifts, such as the polarization drift, may play a comparable or even larger role than the $E_\theta \times B_T$ in the far-SOL. This is left to further studies, as using a single value for each parameter is sufficient to demonstrate the controlling physics of impurity transport within the framework of this reduced model.

We also neglect the impact of magnetic field fluctuations. Magnetic field fluctuations could induce intermittent drifts on the impurity ions similar to the electric field fluctuations described in this paper, but data on magnetic field fluctuations in the SOL is even more scarce/non-existent. This

type of study would be better handled by, e.g., electromagnetic gyrokinetic simulations of the SOL so that fluctuations are better approximated.

b. Prompt Re-deposition of Tungsten

Prompt re-deposition of W ions in the DIVIMP simulations must be included to obtain agreement with TGYRO and 3DLIM. Without this effect, all the DIVIMP calculations of W density (pink lines) in the above figures would be roughly 1-2 orders of magnitude higher and thus would not agree well with TGYRO or 3DLIM at the zone boundaries. This is consistent with ERO simulations, which indicate that for DIII-D divertor conditions the re-deposition fraction is expected to be particularly large (see Fig. 9 and 10 in [24]). For core-edge integration, it is thus desirable to keep $x = \lambda_{iz}/\lambda_{sheath}$ as small as possible by using wall materials with a short λ_{iz} or scenarios in which λ_{sheath} is maximized [25].

V. Conclusions

Successful reactor designs rely on an accurate, physics-based understanding of how impurities radially transport into the core. Our results show that an impurity radial transport paradigm based on fluctuations in E_θ may be able to replace the anomalous diffusion model that has historically been employed. Fluctuations in E_θ results in temporary $v_r = E_\theta \times B_T$ bi-directional impurity ion transport that when coupled with the traditional parallel fluid forces transports W throughout the entire SOL and into the core. For the L-mode discharge studied here, scans in the primary inputs to the model shows that the amount of W penetrating the core is sensitive to the magnitude of the E_θ fluctuation value up until ~1,000 V/m. The results are also particularly sensitive to the probability of a positive fluctuation value, with larger probabilities resulting in less core W contamination. A scan in τ_{corr} finds that the results are sensitive up to around 3 μs, with further increases having a negligible effect on the W density. It was also important to include a prompt re-deposition model for W, otherwise the amount of W within the SOL and core were ~1-2 orders of magnitude higher than the experimentally constrained TGYRO and 3DLIM simulation results. These results suggest that minimizing the transport of impurities across the separatrix and into the core may require:

- Minimizing the magnitude of E_θ fluctuations near the separatrix
- Developing scenarios in which fluctuations in E_θ are preferentially positive/negative when the toroidal magnetic field is counterclockwise/clockwise
- Utilizing wall materials with short λ_{iz}
- Maximizing the width of the sheath, λ_{sheath}

In conclusion, a radial impurity transport model based on fluctuations in E_θ may be used to make more accurate predictions of core impurity contamination in future reactor designs. There is no physics basis from which to assume that values of $D_\perp$ that reproduce measurements in current machines will apply to reactor-scale devices. One can instead use physically justifiable results from simulations of turbulence at the reactor scale to predict and minimize the levels of core impurity contamination. Furthermore, by tying core contamination to measurable phenomena (the statistics of fluctuations in E_θ) operational scenarios can be identified in which either the

magnitude of E_θ is minimized and/or the fluctuations preferentially transport impurity ions away from the core.

VI. Acknowledgements

This material is based upon work supported by the U.S. Department of Energy, Office of Science, Office of Fusion Energy Sciences, using the DIII-D National Fusion Facility, a DOE Office of Science user facility, under Awards DE-FC02-04ER54698, DE-AC05-00OR22725, DE-SC0019256 and DE-FG02-07ER54917.

Disclaimer: This report was prepared as an account of work sponsored by an agency of the United States Government. Neither the United States Government nor any agency thereof, nor any of their employees, makes any warranty, express or implied, or assumes any legal liability or responsibility for the accuracy, completeness, or usefulness of any information, apparatus, product, or process disclosed, or represents that its use would not infringe privately owned rights. Reference herein to any specific commercial product, process, or service by trade name, trademark, manufacturer, or otherwise does not necessarily constitute or imply its endorsement, recommendation, or favoring by the United States Government or any agency thereof. The views and opinions of authors expressed herein do not necessarily state or reflect those of the United States Government or any agency thereof.

VII. Appendix

The codes used in this paper are all contained within the OEDGE suite of codes. The code can be downloaded from the GitHub repository found at the following link: https://github.com/ORNL-Fusion/OEDGE.

VIII. References

1. Stangeby, P. C. *The Plasma Boundary of Magnetic Fusion Devices*. Plasma Physics Series. Bristol ; Philadelphia: Institute of Physics Pub, 2000.
2. Wootton, A. J., H. Y. W. Tsui, and S. Prager. "Edge Turbulence in Tokamaks, Stellarators and Reversed Field Pinches." *Plasma Physics and Controlled Fusion* 34, no. 13 (December 1992): 2023. https://doi.org/10.1088/0741-3335/34/13/035.
3. LaBombard, B. "An Interpretation of Fluctuation Induced Transport Derived from Electrostatic Probe Measurements." *Physics of Plasmas* 9, no. 4 (April 2002): 1300–1311. https://doi.org/10.1063/1.1459060.
4. Kuang, A. Q., S. Ballinger, D. Brunner, J. Canik, A. J. Creely, T. Gray, M. Greenwald, et al. "Divertor Heat Flux Challenge and Mitigation in SPARC." *Journal of Plasma Physics* 86, no. 5 (October 2020): 865860505. https://doi.org/10.1017/S0022377820001117.
5. Romazanov, J., A. Kirschner, S. Brezinsek, R. A. Pitts, D. Borodin, S. Rode, M. X. Navarro, et al. "Beryllium Erosion and Redeposition in ITER H, He and D–T Discharges." *Nuclear Fusion* 62, no. 3 (January 2022): 036011. https://doi.org/10.1088/1741-4326/ac4776.

6. Oliveira, D. S., T. Body, D. Galassi, C. Theiler, E. Laribi, P. Tamain, A. Stegmeir, et al. "Validation of Edge Turbulence Codes against the TCV-X21 Diverted L-Mode Reference Case." *Nuclear Fusion* 62, no. 9 (July 2022): 096001. https://doi.org/10.1088/1741-4326/ac4cde.
7. N. R. Mandell. "Magnetic Fluctuations in Gyrokinetic Simulations of Tokamak Scrape-Off Layer Turbulence." Princeton University, 2021.
8. Holtrop, K., D. Buchenauer, C. Chrobak, C. Murphy, R. Nygren, E. Unterberg, and M. Zach. "The Design and Use of Tungsten Coated TZM Molybdenum Tile Inserts in the DIII-D Tokamak Divertor." *Fusion Science and Technology* 72, no. 4 (November 17, 2017): 634–39. https://doi.org/10.1080/15361055.2017.1347456.
9. Candy, J., C. Holland, R. E. Waltz, M. R. Fahey, and E. Belli. "Tokamak Profile Prediction Using Direct Gyrokinetic and Neoclassical Simulation." *Physics of Plasmas* 16, no. 6 (June 26, 2009): 060704. https://doi.org/10.1063/1.3167820.
10. Zamperini, Shawn, T. Abrams, J. H. Nichols, J. D. Elder, J. D. Duran, P. C. Stangeby, D. C. Donovan, D. L. Rudakov, A. Wingen, and C. Crowe. "Separatrix-to-Wall Simulations of Impurity Transport with a Fully Three-Dimensional Wall in DIII-D." *Fusion Science and Technology* 0, no. 0 (July 15, 2022): 1–10. https://doi.org/10.1080/15361055.2022.2082791.
11. Stangeby, P.C., J.D. Elder, J.A. Boedo, B. Bray, N.H. Brooks, M.E. Fenstermacher, M. Groth, et al. "Interpretive Modeling of Simple-as-Possible-Plasma Discharges on DIII-D Using the OEDGE Code." *Journal of Nuclear Materials* 313–316 (March 2003): 883–87. https://doi.org/10.1016/S0022-3115(02)01470-8.
12. Unterberg, E.A., D.C. Donovan, J.D. Duran, P.C. Stangeby, S. Zamperini, T. Abrams, D.L. Rudakov, W.R. Wampler, and M.P. Zach. "Use of Isotopic Tungsten Tracers and a Stable-Isotope-Mixing Model to Characterize Divertor Source Location in the DIII-D Metal Rings Campaign." *Nuclear Materials and Energy* 19 (May 2019): 358–63. https://doi.org/10.1016/j.nme.2019.02.028.
13. Nichols, J.H., T. Abrams, C.P. Chrobak, D.C. Donovan, J.D. Duran, J.D. Elder, D.L. Rudakov, et al. "Modeling of ExB Effects on Tungsten Re-Deposition and Transport in the DIII-D Divertor." *Nuclear Fusion* 61, no. 9 (September 1, 2021): 096018. https://doi.org/10.1088/1741-4326/ac14e6.
14. Elder, J.D., P.C. Stangeby, E.A. Unterberg, T. Abrams, J.A. Boedo, D. Donovan, A.G. McLean, D.L. Rudakov, W.R. Wampler, and J.G. Watkins. "Evidence of Near-SOL Tungsten Accumulation Using a Far-SOL Collector Probe Array and OEDGE Modelling in the DIII-D Metal Rings L-Mode Discharges." *Nuclear Materials and Energy* 19 (May 2019): 287–94. https://doi.org/10.1016/j.nme.2019.03.007.
15. Watkins, J. G., J. Salmonson, R. Moyer, R. Doerner, R. Lehmer, L. Schmitz, and D. N. Hill. "A Fast Scanning Probe for DIII–D." *Review of Scientific Instruments* 63, no. 10 (October 1992): 4728–30. https://doi.org/10.1063/1.1143621.
16. Abrams, Tyler, Daniel M. Thomas, Ezekial A. Unterberg, and Alexis R. Briesemeister. "Advances in Low-Temperature Tungsten Spectroscopy Capability to Quantify DIII-D Divertor Erosion." *IEEE Transactions on Plasma Science* 46, no. 5 (May 2018): 1298–1305. https://doi.org/10.1109/TPS.2018.2797691.
17. Rooij, G. J. van, J. W. Coenen, L. Aho-Mantila, S. Brezinsek, M. Clever, R. Dux, M. Groth, et al. "Tungsten Divertor Erosion in All Metal Devices: Lessons from the ITER like Wall of JET." *Journal of Nuclear Materials*, Proceedings of the 20th International

Conference on Plasma-Surface Interactions in Controlled Fusion Devices, 438 (July 1, 2013): S42–47. https://doi.org/10.1016/j.jnucmat.2013.01.007.
18. Staebler, G. M., and J. E. Kinsey. "Electron Collisions in the Trapped Gyro-Landau Fluid Transport Model." *Physics of Plasmas* 17, no. 12 (December 16, 2010): 122309. https://doi.org/10.1063/1.3505308.
19. Belli, E. A., and J. Candy. "Kinetic Calculation of Neoclassical Transport Including Self-Consistent Electron and Impurity Dynamics." *Plasma Physics and Controlled Fusion* 50, no. 9 (July 2008): 095010. https://doi.org/10.1088/0741-3335/50/9/095010.
20. Stangeby, P.C., and J.D. Elder. "Calculation of Observable Quantities Using a Divertor Impurity Interpretive Code, DIVIMP." *Journal of Nuclear Materials* 196–198 (December 1992): 258–63. https://doi.org/10.1016/S0022-3115(06)80042-5.
21. Summers, H.P. The ADAS User Manual, (2004) version 2.6 www.adas.ac.uk
22. Nachtrieb, R., and B. LaBombard. "Helium-3 Transport Experiments in the Scrape-off Layer with the Alcator C-Mod Omegatron Ion Mass Spectrometer." *Physics of Plasmas* 7, no. 11 (November 2000): 4573–78. https://doi.org/10.1063/1.1312281.
23. Boedo, J. A., M. J. Schaffer, R. Maingi, and C. J. Lasnier. "Electric Field-Induced Plasma Convection in Tokamak Divertors." *Physics of Plasmas* 7, no. 4 (April 2000): 1075–78. https://doi.org/10.1063/1.873915.
24. Guterl, J., I. Bykov, R. Ding, and P. Snyder. "On the Prediction and Monitoring of Tungsten Prompt Redeposition in Tokamak Divertors." *Nuclear Materials and Energy* 27 (June 2021): 100948. https://doi.org/10.1016/j.nme.2021.100948.
25. Abrams, T., J. G. Guterl, S. Abe, D. C. Donovan, I. Bykov, C. A. Johnson, J. H. Nichols, et al. "Recent DIII-D Progress toward Validating Models of Tungsten Erosion, Re-Deposition, and Migration for Application to next-Step Fusion Devices." *Materials Research Express* 10, no. 12 (December 2023): 126503. https://doi.org/10.1088/2053-1591/ad0f43.
26. McLean, A.G., J.D. Elder, P.C. Stangeby, S.L. Allen, J.A. Boedo, N.H. Brooks, M.E. Fenstermacher, et al. "DIVIMP Modeling of the Toroidally Symmetrical Injection of 13CH4 into the Upper SOL of DIII-D." *Journal of Nuclear Materials* 337–339 (March 2005): 124–28. https://doi.org/10.1016/j.jnucmat.2004.10.130.
27. Zamperini, S.A., J.H. Nichols, P.C. Stangeby, D.C. Donovan, J.D. Duran, J.D. Elder, E.A. Unterberg, and D.L. Rudakov. "The Role of BT-Dependent Flows on W Accumulation at the Edge of the Confined Plasma." *Nuclear Fusion* 62, no. 2 (February 1, 2022): 026037. https://doi.org/10.1088/1741-4326/ac3fe7.
28. Rosenthal, A. M., J. W. Hughes, A. Bortolon, F. M. Laggner, T. M. Wilks, R. Vieira, R. Leccacorvi, et al. "A 1D Lyman-Alpha Profile Camera for Plasma Edge Neutral Studies on the DIII-D Tokamak." *Review of Scientific Instruments* 92, no. 3 (March 2021): 033523. https://doi.org/10.1063/5.0024115.
29. McKee, G., R. Ashley, R. Durst, R. Fonck, M. Jakubowski, K. Tritz, K. Burrell, C. Greenfield, and J. Robinson. "The Beam Emission Spectroscopy Diagnostic on the DIII-D Tokamak." *Review of Scientific Instruments* 70, no. 1 (January 1999): 913–16. https://doi.org/10.1063/1.1149416.
30. D'Ippolito, D. A., J. R. Myra, and S. J. Zweben. "Convective Transport by Intermittent Blob-Filaments: Comparison of Theory and Experiment." *Physics of Plasmas* 18, no. 6 (June 2011): 060501. https://doi.org/10.1063/1.3594609.